



Experiment title: Synthesis of layered titanium phosphate, $\text{Ti}(\text{HPO}_4)_2 \cdot \text{H}_2\text{O}$, at high pressures: An angle dispersive, time-resolved, *in-situ* study using diamond anvil cells and fast area detectors.

Experiment number:
CH-798

Beamline: ID9	Date of experiment: from: 27-10 1999 to: 02-11 1999	Date of report: 26-2 2000
Shifts: 12	Local contact(s): Stefan Carlson and Michael Hanfland	<i>Received at ESRF:</i>

Names and affiliations of applicants (* indicates experimentalists):

Anne Marie Krogh Andersen*, Department of Chemistry, University of Odense, DK-5230 Odense M, Denmark.

Poul Norby*, Department of Chemistry, University of Oslo, N-0315 Oslo, Norway.

Stefan Carlson*, ESRF.

Report:

A series of *in-situ* experiments following the hydrothermal synthesis of the layered phosphate, $\alpha\text{-Ti}(\text{HPO}_4)_2 \cdot \text{H}_2\text{O}$ were performed using a heated high-pressure cell. These experiments show that it is feasible to do accurate studies of chemical reactions in a diamond anvil cell at elevated temperatures, even though the sample size is miniscule.

Time-resolved X-ray diffraction data in angular dispersive mode were collected at ID9 using monochromatic X-ray radiation ($\lambda=0.4362 \text{ \AA}$) with a CCD-based area-detector. The Princeton CCD-detector (supplied by the detector-pool) was equipped with an image intensifier, and the angular- and time-resolution were well suited for the experiments. A schematic diagram of the externally heated diamond cell [1] that was used for the experiments is shown in Figure 1. The pressurized sample chamber in the cell was approximately $250 \mu\text{m}$ in diameter and $80 \mu\text{m}$ in height.

The reaction mixture consisted of amorphous titanium phosphate mixed with 85% phosphoric acid to form a gel. The gel was loaded into the diamond cell with a small ruby for pressure measurements. The temperature was monitored by Cr-Al thermocouples close to the sample, and the pressure by measuring laser-induced fluorescence light of the small ruby in the sample chamber.

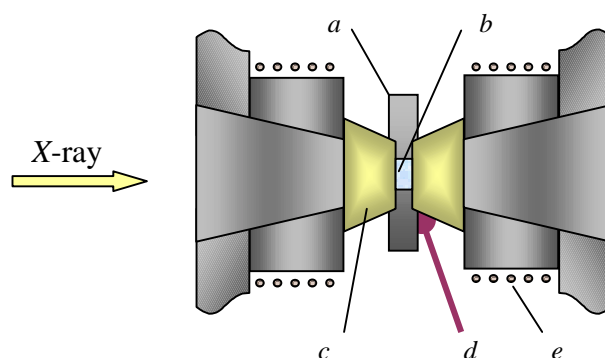


Figure 1. Schematic diagram of the heated diamond cell used. (a) Gasket (b) Sample (c) Diamond anvil (d) Thermocouple (e) Heater-coil.

Using the software FIT2D [2] the images were corrected for spatial distortion, non-linear features in the background, Lorenz factor and polarization before subsequent integration over the entire powder rings. The progress of crystallisation and degradation was estimated from the diffraction patterns by using integrated

intensities of diffraction lines. Well-resolved diffraction lines with no overlap between the two phases were used. A 2θ range was defined around each diffraction peak, and a linear background was defined by using background counts on each side of the peak. The background counts were subtracted from the total counts over the 2θ range to give the net integrated intensity. The integrated intensities of the selected reflections from each phase were added and normalised to represent the percentage of crystallinity (α).

Figure 2a is a 3-dimensional representation of the diffraction profiles as a function of time during the crystallisation of $\alpha\text{-Ti}(\text{HPO}_4)_2 \cdot \text{H}_2\text{O}$ at 170°C and 2.5 GPa. In Figure 2b normalised integrated intensities of diffraction lines of $\alpha\text{-Ti}(\text{HPO}_4)_2 \cdot \text{H}_2\text{O}$ are plotted as a function of time (t). The crystallisation curve has been fitted using a first order Avrami-type rate equation, $\alpha=100(1-\exp(-k(t-t_0)))$, where k is a rate constant and t_0 is the starting time of the crystallisation. The fitted values became $k = 0.49 \text{ min}^{-1}$ and $t_0 = 1.49 \text{ min}$.

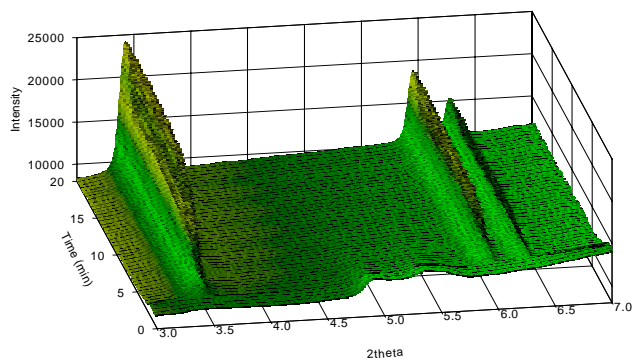


Figure 2a. 3D representation of the crystallisation of $\alpha\text{-Ti}(\text{HPO}_4)_2 \cdot \text{H}_2\text{O}$ from an amorphous gel.

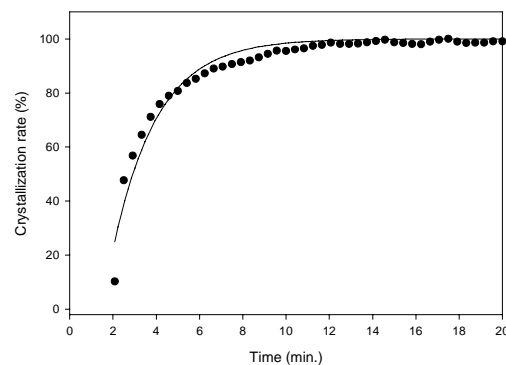


Figure 2b Crystallisation curve for $\alpha\text{-Ti}(\text{HPO}_4)_2 \cdot \text{H}_2\text{O}$

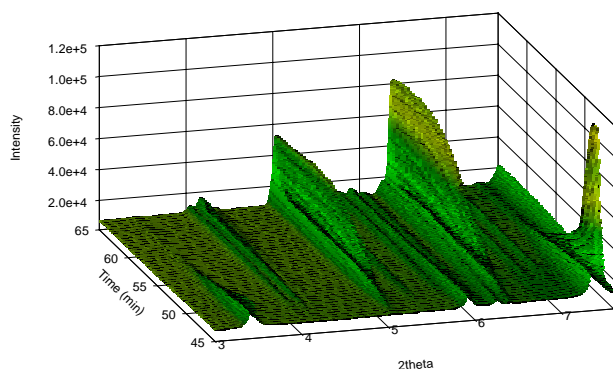


Figure 3a. Conversion of $\alpha\text{-Ti}(\text{HPO}_4)_2 \cdot \text{H}_2\text{O}$ to new phase

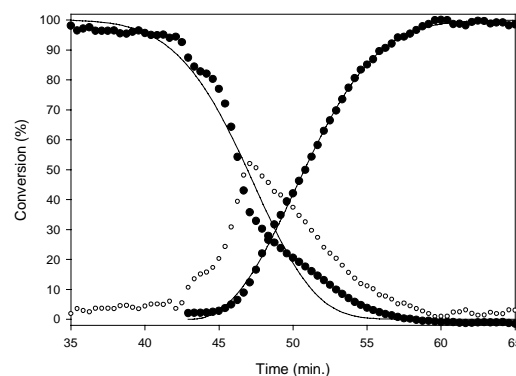


Figure 3b Crystallisation and degradation curves for the conversion of $\alpha\text{-Ti}(\text{HPO}_4)_2 \cdot \text{H}_2\text{O}$ to new phase.

At 220°C and 0.8 GPa alpha transform to a new phase. In Figure 3a the 3D plot of the conversion from $\alpha\text{-Ti}(\text{HPO}_4)_2 \cdot \text{H}_2\text{O}$ to the new phase is shown. The crystallisation curve (Figure 3b) was fitted, using least-squares methods, with a modified Avrami expression [3] $\alpha=100(1-\exp(-(k(t-t_0))^n))$ and a similar expression for the degradation $\alpha=100\exp(-(k(t-t_0))^n)$, where k and t_0 has the same meaning as above. The parameter n is

connected to the mechanism of nucleation and crystallisation. It can clearly be seen that the crystallisation of the new phase is fitted well by the modified Avrami expression. However, the degradation of $\alpha\text{-Ti}(\text{HPO}_4)_2 \cdot \text{H}_2\text{O}$ does not follow the empirical expression. This can be due to an amorphous phase or structural transformations of $\alpha\text{-Ti}(\text{HPO}_4)_2 \cdot \text{H}_2\text{O}$ during degradation. The deviation from ideal behavior (degradation+crystallisation=100%) is shown with open circles in Figure 3b. Fitted values to the Avrami expression became, $k(\text{degr}) = 0.055 \text{ min}^{-1}$, $n(\text{degr}) = 5.23$, $k(\text{cryst}) = 0.109 \text{ min}^{-1}$ and $n(\text{cryst}) = 2.36$.

[1] W. A. Bassett, A. H. Shen, M. Bucknum and I-Ming Chou, *Rev. Sci. Instrum.* **64** (1993) 2340.

[2] A. Hammersley, FIT2D V10.3 Reference Manual V4.0, ESRF, Grenoble, France, 1998.

[3] P. Norby, A. N. Christensen and J. C. Hanson, *Inorg. Chem.* **38** (1999) 1216.